JACS
JOURNAL OF THE AMERICAN CHEMICAL SOCIETY
pubs.acs.org/JACS
Article

Hydrogen-Bond Network Promotes Water Splitting on the TiO_2 Surface

Xiaochuan Ma, Yongliang Shi, Jianyi Liu, Xintong Li, Xuefeng Cui, Shijing Tan,* Jin Zhao,* and Bing Wang*

Cite This: *J. Am. Chem. Soc.* 2022, 144, 13565−13573
Read Online
ACCESS | Metrics & More | Article Recommendations | Supporting Information

ABSTRACT: Breaking the strong covalent O−H bond of an isolated H_2O molecule is difficult, but it can be largely facilitated when the H_2O molecule is connected with others through hydrogen-bonding. How a hydrogen-bond network forms and performs becomes crucial for water splitting in natural photosynthesis and artificial photocatalysis and is awaiting a microscopic and spectroscopic understanding at the molecular level. At the prototypical photocatalytic H_2O/anatase-TiO_2(001)-(1×4) interface, we report the hydrogen-bond network can promote the coupled proton and hole transfer for water splitting. The formation of a hydrogen-bond network is controlled by precisely tuning the coverage of water to above one monolayer. Under ultraviolet (UV) light irradiation, the hydrogen-bond network opens a cascaded channel for the transfer of a photoexcited hole, concomitant with the release of the proton to form surface hydroxyl groups. The yielded hydroxyl groups provide excess electrons to the TiO_2 surface, causing the reduction of Ti^{4+} to Ti^{3+} and leading to the emergence of gap states, as monitored by *in situ* UV/X-ray photoelectron spectroscopy. The density functional theory calculation reveals that the water splitting becomes an exothermic process through hole oxidation with the assistance of the hydrogen-bond network. In addition to the widely concerned exotic activity from photocatalysts, our study demonstrates the internal hydrogen-bond network, which is ubiquitous at practical aqueous/catalyst interfaces, is also indispensable for water splitting.

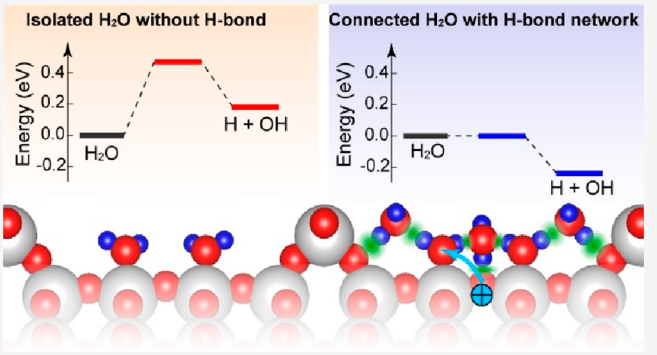

INTRODUCTION

Water splitting serves as the elementary step in natural photosynthesis to harvest solar energy and thus has been recognized as one of the most important chemical reactions on Earth.[1,2] Down to the molecular level, water splitting initiates from the breaking of a covalent HO−H bond, which is thought to be challenging because of the high bond energy of ∼492 kJ/mol (5.10 eV). In an aqueous environment, as described by the Grotthuss mechanism,[3] concomitant cleavage and formation of covalent O−H bonds in adjacent H_2O molecules can be facilitated by the intermolecular hydrogen bond (H-bond). Undoubtedly, the weak H-bond is ubiquitous and plays a key role in water chemistry. Recent scanning tunneling microscopy (STM) studies in real space have revealed that the H-bond can drive the sequential H atom relay reaction in a water chain,[4] direct the quantum tunneling of a proton in a water cluster,[5] and assist the interfacial and intermolecular H atom transfer.[6−8] Obviously, in these processes the H_2O molecules behave as a "pseudodissociated" state,[9,10] since the O−H bonds are reversibly breaking and re-forming without yielding separated hydroxyl groups. However, to complete water splitting, even for a single H_2O molecule, it requires gaining reactivity from a catalyst to proceed via $H_2O \rightarrow OH^- + H^+$[11,12] or gaining energy from charge transfer to proceed with either electron reduction via $H_2O + e^- \rightarrow OH^- + H$[13,14] or hole oxidation via $H_2O + h^+ \rightarrow {}^{\bullet}OH + H^+$.[14,15]

In photocatalytic water splitting,[16] hole oxidation is the rate-determining step toward oxygen evolution by a semiconductor catalyst.[17] How to promote the transfer of photoexcited holes from the catalyst to H_2O molecules becomes crucial and has been extensively researched.[18] On the model photocatalyst TiO_2 surfaces, hole transfer is dependent on the alignment between the highest occupied molecular orbitals (HOMOs) of water and the valence band maximum (VBM) of TiO_2.[19,20] In real space, the photoexcited holes are self-trapped to the lattice O sites, forming O^- small polarons,[21,22] while the H_2O adsorbs at the Ti cation sites, which causes spatial isolation to prevent direct hole transfer. Nevertheless, it has been suggested that the interfacial H-bond can promote the hole transfer and thus

Received: April 6, 2022
Published: July 19, 2022

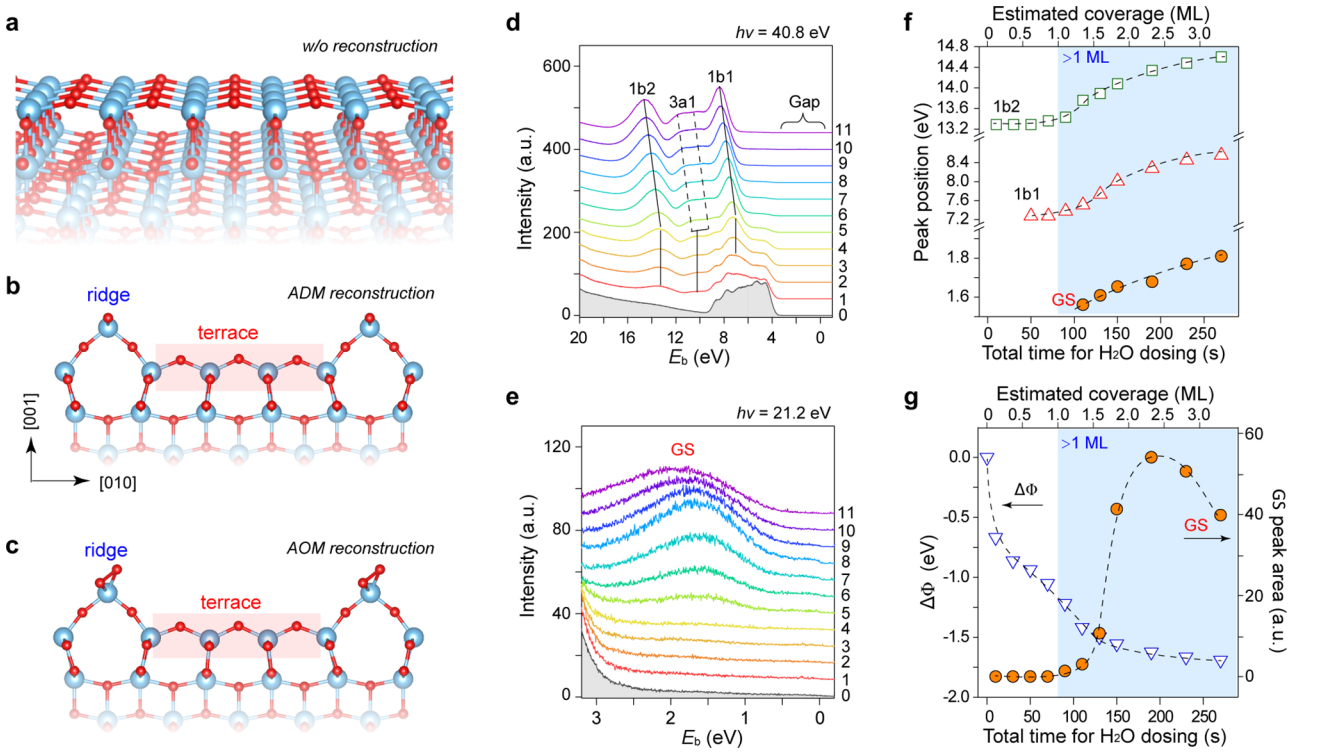

Figure 1. Emergence of GS at the anatase-TiO_2(001)-(1×4) surface with increasing water coverage at 90 K. (a) Model of the (1×1) surface of anatase-TiO_2(001) without reconstruction. (b, c) Reconstructed (1×4) surfaces with ADM and O-rich AOM modes, respectively. (d) Survey UPS spectra obtained at the bare anatase-TiO_2(001)-(1×4) surface (spectrum 0) and after sequential water adsorption (spectra 1 to 11), excited by $h\nu$ = 40.8 eV at 90 K. The numbers record the dosing times, and each dosing involves water exposure at 1 × 10^{-9} mbar for 20 s. The spectra are vertically offset for clarity. (e) Spectra simultaneously obtained with $h\nu$ = 21.2 eV excitation, highlighting the spectral changes in the gap. (f) Peak positions of $1b_1$ and $1b_2$ in (d) and a GS in (e), plotted as a function of H_2O dosing time. (g) Intensity of the GS (right ordinate) and the work function change (left ordinate), plotted as a function of H_2O dosing time. The top axis is the estimated coverage with the dosing time of 80 s corresponding to 1 ML (see Methods). The dashed lines guide the eye. The blue shades indicate the area with H_2O coverage >1 ML.

increase the oxidation efficiency of water[23] or methanol.[24] We have recently revealed that the H-bond can strongly couple the hole transfer to the quantum proton motion at the methanol/TiO_2 interface on the basis of the nuclear quantum effects of the light H atoms.[25] These results provide insights to interrogate the roles of the H-bond network in water splitting, while an accurate control of the intermolecular and interfacial H-bond network formation is highly demanded in experiments.

On the widely studied rutile-TiO_2(110) surface, we reported the photocatalytic dissociation of H_2O monomers at the stoichiometric Ti_{5c} sites by using STM.[14] The Yang group found the single H-bond in the water dimer enhances the water dissociation, while one-dimensional H-bonds in water chains inhibit the reaction.[26,27] Recently, we reported that the interfacial H-bond can facilitate the dehydrogenation of H_2O at <1 monolayer (ML) coverage by STM.[7] Since the weak H-bonds are easily disturbed by the STM tip,[7] spectroscopic techniques are necessary to characterize the role of H-bonds instead of STM. Hussain et al. studied the ordered hydroxyl and water structures at a liquid water/TiO_2 interface by X-ray diffraction, where the formation of hydroxyl is caused by the mixed adsorption of O_2 and H_2O on a partially defected surface.[28] Kamal et al. reported the local H-bonding configuration in D_2O/OD at the rutile-TiO_2(110) surface in the submonolayer and monolayer regime by X-ray photoelectron spectroscopy (XPS).[29] However, the role of the H-bond network in photoexcited water splitting on the rutile-TiO_2(110) surface has not been revealed yet. One of the challenges is that the intrinsic defects of surface oxygen vacancies[30] and subsurface Ti interstitials,[31] as well as the bridging hydroxyl groups[32] produced by either spontaneous or photocatalytic water dissociation, generate similar Ti^{3+} gap states (GS) at ∼0.9 eV below the Fermi level (E_F),[30,31,33,34] making it quite difficult to distinguish them. Here, to minimize the effect of intrinsic defects, we employ the fully oxidized anatase-TiO_2(001) surface to investigate the promotion effect of the H-bond network in water splitting.

The low-index anatase-TiO_2(001) surface is believed to possess high reactivity,[18,35,36] and diverse nano- and micrometer-sized anatase-TiO_2 crystals have been synthesized for catalytic applications.[37,38] The high reactivity of the synthesized TiO_2 particles originates from the high surface energy of {001} facets. However, surface science studies with ultrahigh vacuum (UHV) treatments inevitably cause the release of surface energy, leading to the (1×4) surface reconstruction with the ridges hunching up on the flat terrace[39−42] (Figure 1a−c). Consequently, plenty of studies disputed the structures and activities of ridge sites,[42−47] but missed the vast expanse of terrace sites that are even more relevant to practical catalytic applications. Regarding water dissociation on the anatase-TiO_2(001)-(1×4) surface, Gong et al. predicted the spontaneous dissociation of H_2O at ridge sites with the breaking of a surface Ti−O bond by using molecular dynamics simulations.[36] Later, Blomquist et al. reported a mixture of dissociated and molecular water phases at ridge sites at 170 K by using XPS.[44] Beinik et al. reported the dissociatively

https://doi.org/10.1021/jacs.2c03690
J. Am. Chem. Soc. 2022, 144, 13565−13573

adsorbed H_2O at ridge sites resulting in a (3×4) periodic structure of hydroxyl pairs at 120 K by using XPS and STM.[42] Yuan et al. observed the twin-protrusion features at ridge sites after exposure to water vapor at 700 °C by *in situ* transmission electron microscopy, which were assigned to paired OH−H_2O groups at the ridge.[47] These results concerned the intrinsic reactivity of the ridge sites for water dissociation but with quite different interpretations of the structures. Also, in these measurements the participation of the high-energy photon flux and electron beam in water dissociation has been largely overlooked. Moreover, in such spontaneous water dissociation, one may find the ridge sites behave as "reactants", rather than "photocatalysts", because the ridge Ti−O bonds are broken and consumed. So far, where and how the photoexcited water splitting can take place on the anatase-TiO_2(001)-(1×4) surface is still unknown.

Our study reveals the terrace sites of the anatase-TiO_2(001)-(1×4) surface can be photoactive and the H-bond network is indispensable for water splitting. The initial step of photoexcited H_2O splitting is evidenced from the hydroxyl group induced GS at ∼1.6 eV below the Fermi level (E_F), as monitored by *in situ* UV photoelectron spectra (UPS). Coverage-dependent experiments indicate the GS starts to arise at >1 ML. Density functional theory (DFT) calculations suggest that the extra H_2O molecules adsorbed above 1 ML can bridge the surface O sites and the H_2O at Ti^{4+} sites to form a H-bond network, providing a cascaded channel for the transfer of photoexcited holes to H_2O, concomitant with the proton transfer to the TiO_2 surface, to fulfill the water splitting.

RESULTS AND DISCUSSION

Emergence of a Gap State. We first revisit the structures of the anatase-TiO_2(001) surface. UHV annealing of the epitaxial grown anatase-TiO_2(001) single-crystalline thin film leads to the (1×4) reconstruction, forming ridge rows with a periodicity four times the lattice constant, as described by the "ad-molecule" model (ADM, Figure 1b).[39,41] Further annealing under a high O_2 partial pressure may cause the formation of an O-rich surface with additional ad-oxygen atoms to the ridges, as more adapted to the "ad-oxygen" model (AOM, Figure 1c).[40,48] In both of the ADM and AOM models, the flat terraces have nearly the same structures involving 5-fold-coordinated Ti_{5c} and 2-fold-coordinated O_{2c} atoms. Our recent study suggests the ADM and AOM may coexist at the surface.[45,49] Despite the different reconstructed ridge geometries in ADM and AOM, our attention below is focused on the terrace sites whose structure may be largely similar to the unreconstructed anatase-TiO_2(001). However, unlike the relatively "flat" rutile-TiO_2(110) surface, the corrugated ridges on the reconstructed structure of anatase-TiO_2(001)-(1×4) make it difficult to recognize the hydroxyl groups and even the water molecules by STM.[40] To overcome this difficulty, we investigate the electronic states by *in situ* UPS/XPS spectra.

We investigate the evolution of electronic states with water on anatase-TiO_2(001)-(1×4) surface by using *in situ* UPS at 90 K. In the survey spectra (Figure 1d), the state in the gap region is too weak to be clearly seen (Figure S1). But intriguingly, the zoom-in spectra within the gap region indicate the appearance of a GS with a binding energy, E_b, at ∼1.6 eV below E_F upon water adsorption (Figure 1e and Figure S1). It can be learned from previous experimental and theoretical studies that the ADM ridges are reactive for spontaneous (not photoexcited) water dissociation,[36,42,44] but do not contribute to a GS in UPS spectra,[42] while the O-rich AOM ridges are quite inert.[40] Therefore, the emergence of a GS could be most probably assigned to the water splitting at terrace sites.

To validate this assignment, we analyze the valence band spectra in more detail. Spectrum 0 is obtained from the bare anatase-TiO_2(001)-(1×4) surface, which mainly presents the distribution of the O-contributed valence bands with E_b ranging from 3.5 to 9.0 eV. Then, sequential water dosing causes the arising of new peaks at $E_b \approx 7.3$, 10.2, and 13.5 eV from spectrum 1 and become remarkable at higher water coverage from spectrum 4. These peaks can be assigned to the three HOMOs of $1b_1$, $3a_1$, and $1b_2$ of water, respectively.[50,51] Clearly, a continuous shift of the peaks to higher binding energies starts from spectrum 4 or spectrum 5 (Figure 1d), where the peak positions are plotted as a function of water dosing time (Figure 1f). Such an energy shift vs coverage can be ascribed to the final-state screening effect, which commonly takes place after the first water layer is fully filled on metal or oxide surfaces.[50,51] Therefore, the turning point between spectrum 4 and spectrum 5 makes a rational estimation of the water coverage of ∼1 ML. Considering a roughly linear increase of water coverage vs the increase of dosing time, we plot the estimated water coverage in the top axis in Figure 1f,g to correlate the peak energy and the coverage.

Meanwhile, the GS, which is undetectable at the bare surface, starts to show up at >1 ML water coverage (Figure 1e). The E_b of the GS also shifts higher (Figure 1f), and its intensity reaches a maximum around spectrum 9 and then decreases at much higher coverage (Figure 1g), where the decrease might be caused by the limited escaping depth of photoelectrons when the ice layer becomes too thick. Water adsorption also reduces the surface work function (Φ) dramatically by ∼1.5 eV from 0 to 1 ML and gently at >1 ML (Figure 1g and Figure S2).

Origin of a Gap State from Photoexcited Water Splitting. The GSs have been observed at defective anatase-TiO_2(001) surfaces produced by Ar^+ sputtering[40] or high-flux UV irradiation.[52,53] Here, the oxidized anatase-TiO_2(001) surface is employed to minimize the defects without a detectable GS.[40] Therefore, the appearance of the GS after water adsorption may suggest the formation of hydroxyl groups from water splitting, similar to the case on rutile-TiO_2(110).[32] To understand this, we first exam whether the water splitting is a photoexcited process during UPS measurements or a spontaneous dissociation[36,42,44] before UPS measurements. It is known that annealing to 230 K can desorb the water molecules[42,54] (Figure S3) and leave the hydroxyls and H atoms at the surface. On this basis, we design three samples with an initial coverage of ∼2 ML H_2O at 90 K: sample 1 is annealed directly to 230 K without UV exposure; sample 2 and sample 3 are exposed to the UV ($h\nu$ = 21.2 eV) for 1 and 60 min, respectively, and then annealed to 230 K (Figure 2a). It can be seen that the GS does not appear at sample 1, but clearly shows up in the other two samples. The comparison results undoubtedly confirm the UV exposure is responsible for the water splitting, while even 230 K annealing of sample 1 cannot form a GS through thermally driven dissociation.

In addition to the GS, a sharp contribution appears just below the E_F (black arrow in Figure 2a) with a parabolic dispersion in the 2D $E_b(k_{||})$ maps (Figure 2b). This feature can be assigned to the metallic state (MS) formed by electron doping at the anatase-TiO_2(001) surface.[52,53] The produced H defects from water splitting provide excess electrons to form a

https://doi.org/10.1021/jacs.2c03690
J. Am. Chem. Soc. 2022, 144, 13565−13573

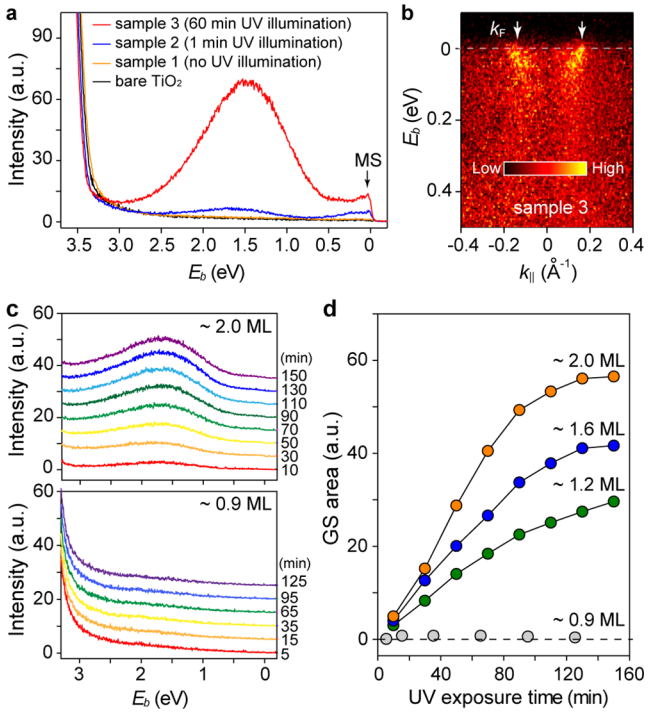

Figure 2. Origin of the gap state from photoexcited water splitting. (a) Three samples with initial H_2O coverage of ~2 ML at 90 K were subjected to 0 min (orange), 1 min (blue), and 60 min (red) UV exposure, respectively. The spectra were obtained after annealing the samples to 230 K. (b) 2D $E_b(k_{||})$ maps obtained at sample 3, indicating the parabolic dispersions of MS. The dark contrast at $k_{||} = 0$ is due to the forbidden photoemission by the matrix element effect. (c) Change of the GS at two samples with ~2.0 and 0.9 ML H_2O, respectively, with increasing UV ($h\nu$ = 21.2 eV) exposure time. (d) Intensity changes of GS (integrated peak area) plotted as a function of UV exposure time at four samples with a H_2O coverage of ~2.0, 1.6, 1.2, and 0.9 ML, respectively, where the coverage is controlled by the dosing time according to Figure 1f.

confined electron gas at the surface region. Considering the 2D Luttinger volume, we can estimate the electron density of $n_{2D} \approx 4.1 \times 10^{13}$ cm^{-2} within the wavevector $k_F = (0.16 \pm 0.02)$ Å^{-1}, via $n_{2D} = k_F^2/2\pi$, at sample 3 with 60 min UV irradiation. Note, the feature of the MS only appears at the 230 K-annealed samples (Figure 2a), but is not that clear in the unannealed samples (Figure 1d,e), since the residual H_2O molecules, which have not been removed by annealing, could largely diminish the electron gas.

One may argue whether the GS in Figure 2a comes from UV-irradiation-induced surface defects[52,53] or really from photoexcited water splitting. To dispel the doubts, we measure the change of GS as a function of UV exposure time with different water coverages of 2.0, 1.6, 1.2, and 0.9 ML (Figure 2c,d). It is clear that a longer UV exposure time could increase the GS intensity, and also the higher the H_2O coverage, the higher the water dissociation rate. But in sharp contrast, measurements conducted at the sample with ~0.9 ML water coverage do not show any GS intensity change (Figure 2c). These results confirm two points: the UV-irradiation-induced surface defects[52,53] are negligible at a ~0.9 ML water covered surface; the photoexcited water splitting can only take place when the coverage is >1 ML, in line with the observation in Figure 1e.

Ti^{3+} Nature of the Gap State from Hydroxyl Groups at Terrace Sites. The electron doping can reduce the Ti^{4+} to the Ti^{3+} state, which can be evidenced from the change of the Ti 2p signal (Figure 3a). At the bare surface, Ti^{4+} contains two

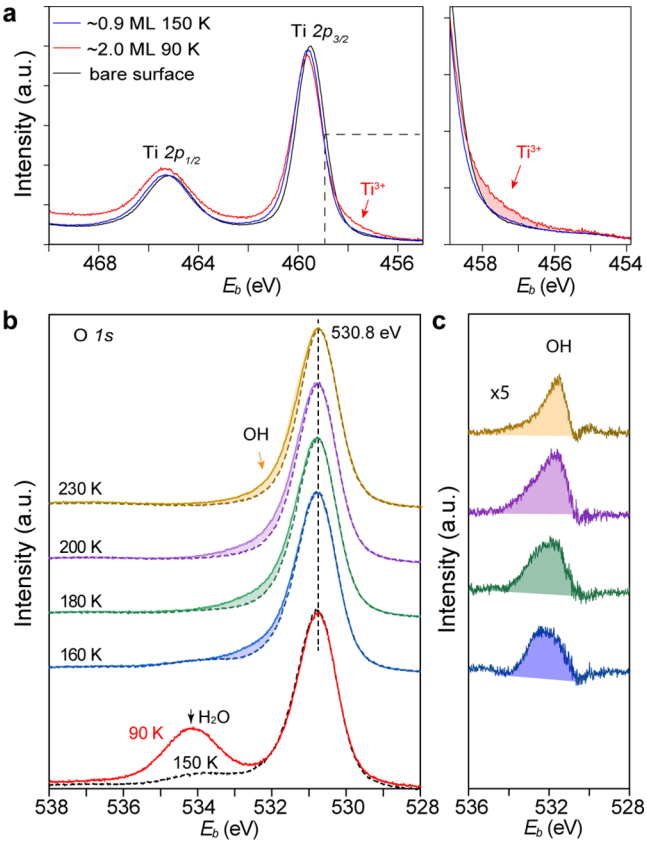

Figure 3. Ti^{3+} nature of the gap state from hydroxyl groups. (a) Ti 2p spectra obtained at the bare surface, ~0.9 ML H_2O covered surface prepared at 150 K, and ~2 ML H_2O covered surface prepared at 90 K, respectively, using Mg Kα excitation. The area marked by the dashed rectangle is magnified in the right panel showing the reduced Ti^{3+} signal (red shaded). (b) Extracting the shoulder signal in O 1s spectra for OH. Sample A is prepared at 90 K with multilayer H_2O adsorption (solid red); sample B is prepared at 150 K with ~0.9 ML H_2O adsorption (dashed black). Both samples are irradiated by $h\nu$ = 21.2 eV for 1 h and then sequentially annealed to higher temperatures of 160, 180, 200, and 230 K to desorb water molecules to extract the contribution of OH. The solid lines are obtained at sample A and the dashed line at sample B. (c) Difference spectra from (b), with an amplification factor of 5. The color shaded areas indicate the differences for the signal of OH.

peaks of Ti $2p_{3/2}$ at ~459.5 eV and $2p_{1/2}$ at ~465.3 eV. Clearly, at the ~2 ML water covered surface, a shoulder at ~457.5 eV arises for the peak of $2p_{3/2}$ (red shaded in Figure 3a) after photoirradiation, which strongly supports the reduced Ti^{3+} nature of the GS from the yielded hydroxyl groups.

Direct evidence for the formation of hydroxyl groups should come from the change of O 1s spectra (Figure 3b). Usually, the hydroxyl groups make a weak contribution as a small shoulder to the intense O 1s peak of the anatase-TiO_2(001) surface, which could be extracted by the XPS peak fitting.[42] Typical O 1s spectra obtained at the bare surface, with H_2O adoption and after UV irradiation, are shown in Figure S4. The peaks were normalized according to the lattice O 1s peak of the bare anatase-TiO_2 for the surface at various H_2O coverages.

https://doi.org/10.1021/jacs.2c03690
J. Am. Chem. Soc. 2022, 144, 13565−13573

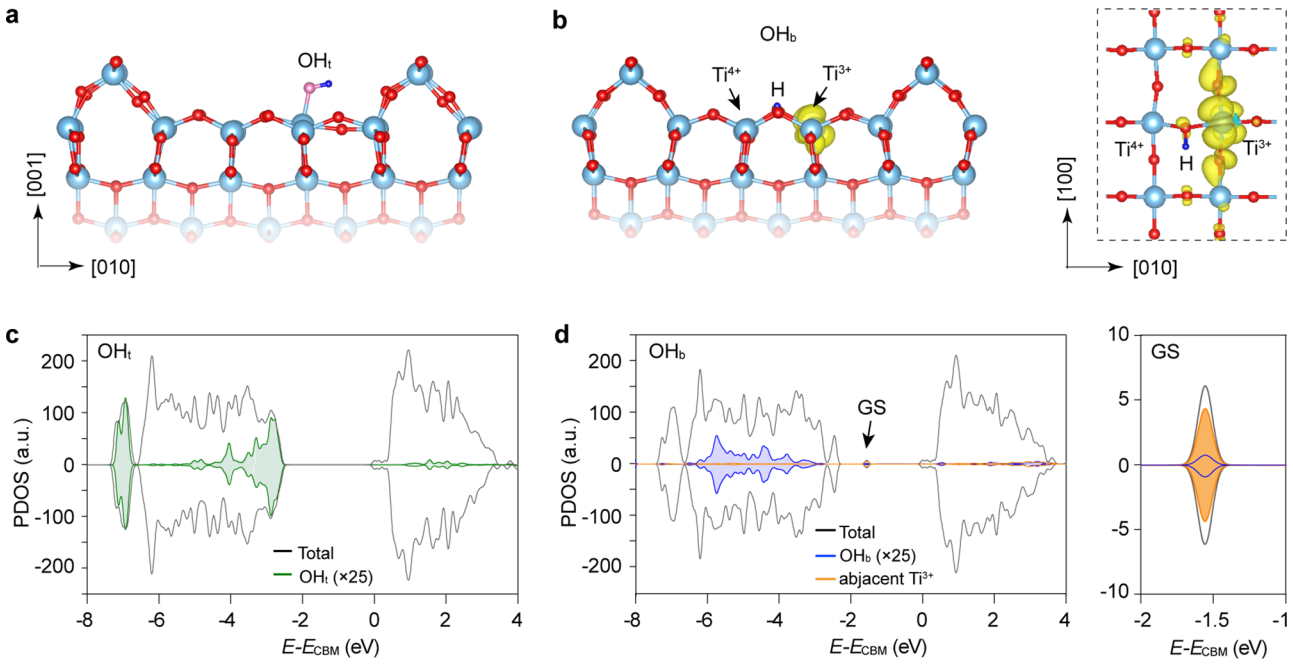

Figure 4. Calculated Ti^{3+} GS of hydroxyl groups at terrace sites. (a, b) Side views of the geometries of OH_t and OH_b, respectively. The yellow indicates the distribution of GS at the OH_b adjacent Ti^{3+} site. The right panel shows the top view of the distribution of GS. (c, d) Calculated total (black) and partial DOS for the hydroxyl groups of OH_t (green) and OH_b (blue), respectively. The DOS in the gap in (d) is enlarged in the right panel. The orange shading highlights the GS at the adjacent Ti^{3+}.

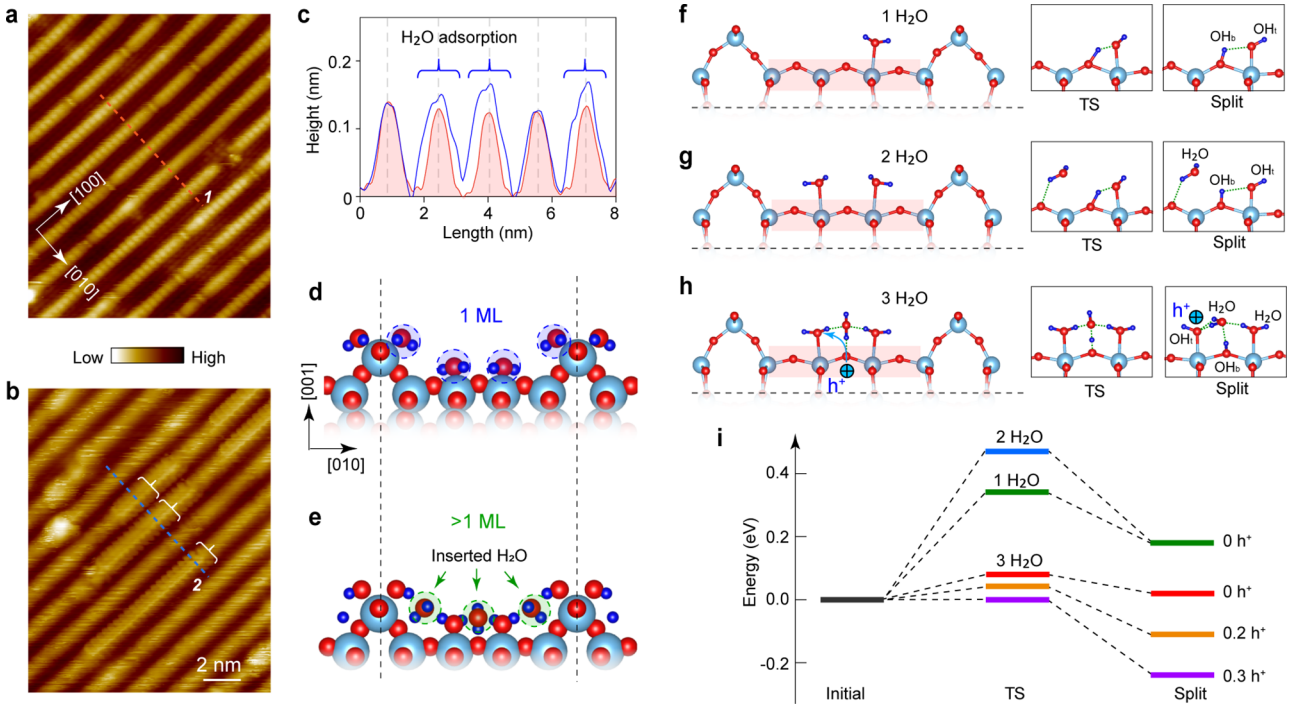

Figure 5. H-bond network formation and the calculated pathways for water splitting. (a) Atomically resolved STM image of a bare anatase-TiO_2(001)-(1×4) surface, acquired at 1.0 V, 10 pA, and 80 K. (b) STM image of the water-adsorbed surface, acquired at 1.2 V, 10 pA, and 80 K. The fuzzy scratches indicate the moving H_2O molecules. The brackets indicate the assembled H_2O structures. (c) Line profiles extracted from the STM images of bare and water-covered surfaces along the lines, distinguished by red and blue, respectively. (d) Proposed adsorption structure of 1 ML water, as two H_2O molecules at a ridge and two H_2O molecules at a terrace in the a (1×4) lattice. (e) Structure of >1 ML water with additional inserted molecules, where the H-bond network forms. (f–h) Simulated water splitting pathways at a terrace, by considering $1H_2O$, $2H_2O$, and $3H_2O$ configurations. (i) Calculated potential energy surface (PES) along the H_2O splitting pathways in (f)–(h), respectively. In the $3H_2O$ configuration, putting holes in H_2O (removing electrons from the $1b_1$ orbital) can effectively reduce the energy barrier.

By fitting the peaks, the contents of O from the OH groups relative to those from the adsorbed water molecules can be obtained. By using XPS peak fitting, we can distinguish the major peak at 530.8 for TiO_2, the peak at ~534.2 eV for

https://doi.org/10.1021/jacs.2c03690
J. Am. Chem. Soc. 2022, 144, 13565−13573

molecular H_2O, and the shoulder peak at 532.2 eV for OH. It is seen that the OH species can be negligible at the ∼1 ML water surface, while the OH groups are at 6% relative to ∼4 ML H_2O after 1 h of UV irradiation. Such quantitative analyses may involve an inaccuracy because the OH production mainly appears at the interface and the XPS attenuation effect appears in the thick water layer.

It was observed that the spontaneous water dissociation at ridges may also contribute to the shoulder peak in O 1s peak.[42] However, such behavior is not obvious at our oxidized anatase-TiO_2(001) surface. This is helpful for us to design an experiment to directly extract the net change of the O 1s signal for water splitting at the terrace. Temperature-dependent experiments determine that multilayer H_2O will desorb at >140 K[54] (Figure S3). Therefore, a sample prepared at ∼150 K will not involve multilayer H_2O and is not expect to generate hydroxyl groups at the terrace, as examined by the absence of a Ti^{3+} signal (Figure 3a). In this context, comparing the samples prepared at ∼90 K (>1 ML H_2O) and ∼150 K (<1 ML H_2O) could certainly distinguish the net change of O 1s signals for hydroxyl groups at the terrace, as shown in Figure 3b. Both the samples are irradiated by UV for 1 h and then sequentially annealed to higher temperatures of 160, 180, 200, and 230 K, respectively. The annealing procedure is aimed at removing the 534.2 eV peak signal from the unreacted H_2O molecules and highlighting the O 1s signals for hydroxyl groups. Clearly, the color shaded spectral difference in Figure 3b could be the net contribution of hydroxyl groups from photoexcited water splitting at terraces. Further analyzing the residual peak of the OH groups after removal of H_2O molecules (Figure 3c) gives the OH coverage of about 0.35 to 0.25 ML from 160 to 230 K, which is close to the estimated OH content by fitting the OH peak above (Figure S4). In addition, similar experimental procedures are conducted to extract the 1π and 3σ orbitals of hydroxyl[42] simultaneously in UPS spectra (Figure S5), to further support the formation of hydroxyl groups.

We next perform the spin-polarized DFT calculation to understand the electronic structures of the hydroxyl groups at terrace sites. The splitting of a H_2O molecule produces two kinds of hydroxyl groups: the OH bonding with a surface Ti atom and the H atom to a bridging O atom, which are denoted as OH_t and OH_b, respectively. The calculated partial density of state (pDOS) shows no GS for OH_t (Figure 4a,c), but a clear GS for OH_b located at about 1.56 eV below the conduction band minimum (Figure 4b,d). The spatial distribution with the spin density of the GS confirms that the excess electrons from OH_b redistribute to an adjacent Ti ion, which is reduced to Ti^{3+}, accompanied with asymmetric structural distortions (Figure 4b and Figure S6). The local structural distortion around OH_b implies the formation of a small electron polaron.[21,22] A similar GS of OH_b with a Ti^{3+} distribution has been realized on the rutile-TiO_2(110) surface.[32]

Formation of a H-Bond Network and Its Role in Photoexcited Water Splitting. Looking back to the valence band spectra in Figure 1d, the $3a_1$ peak of the water HOMO is obviously broadened and splits into two peaks, as indicated by the dashed lines at the >1 ML coverage. The splitting of the $3a_1$ peak can be more clearly seen in the 2D second derivative angle-resolved $E_b(k_{||})$ maps, which forms two nondispersive bands (Figure S7). The splitting of the $3a_1$ peaks has been recognized as the signature for H-bond network formation at high coverage, implying two kinds of H_2O molecules that act as the H-donor and H-acceptor, respectively.[51,55] We further look for evidence of H-bond network formation in real space by using STM (Figure 5a,b). Our previous STM study has observed H_2O adsorption and dissociation at the point defects with a low coverage.[40] But at the nondefective ridge and terraces sites, the STM images become extremely fuzzy (Figure 5b and Figure S8), indicating the H_2O molecules are quite mobile and easily disturbed by the STM tip. When close to a monolayer, the H_2O molecules start to self-assemble into ordered structures (brackets labeled in Figure 5b and Figure S8c). Line profiles extracted at the clean TiO_2 surface and across the ordered H_2O structures (red and blue in Figure 5c) indicate that H_2O-induced contrast can spread from ridge to terrace. A close look at the ordered structures in Figure 5b suggests that four H_2O molecules may adsorb in a (1×4) lattice. On the basis of these analyses, we construct the configuration of 1 ML H_2O by DFT as two H_2O molecules bonding to Ti at a ridge and the other two to Ti at a terrace in each (1×4) lattice (Figure 5d and Figure S9). Our DFT calculations suggest the molecular H_2O at 1 ML coverage can be maintained at both the ridge and terrace sites with an average adsorption energy of 0.64 eV/molecule (Figure S9g). The small adsorption energy of H_2O at terrace sites implies it is physically absorbed and quite unstable. The unstable physisorption of H_2O molecules at terrace sites has also been suggested by Selçuk and Selloni, with an adsorption energy of 0.63 eV/molecule at full coverage.[56]

The most interesting thing is that the photoexcited water splitting at the terrace could only be observed at >1 ML coverage; that is, the additional H_2O molecules after the first monolayer is fully occupied can effectively promote the water splitting. DFT optimization suggests the additional H_2O molecules can insert into the first layer, reducing the O−O distance to form H-bond networks (Figure 5e). The inserted H_2O molecules introduce additional intermolecular interactions that can stabilize the H_2O configuration by increasing the averaged adsorption energy to 0.71 eV/molecule (Figure S9h). The stability of the proposed configuration has been further verified by the *ab initio* molecular dynamics (AIMD) simulations with the trajectory length of 10 ps at a temperature of 100 K (Figure S10a−c). The simulation further confirms the proposed configuration is still stable with additional water layers as in aqueous environments (Figure S10d−f). To focus on the H_2O splitting on the terrace, we compare the energy barriers from the calculated potential energy surfaces (PESs) with $1H_2O$ and $2H_2O$ at terrace Ti^{4+} sites and with an additional inserting H_2O molecule (i.e., $3H_2O$), to mimic the <1 ML, 1 ML, and >1 ML coverages, respectively (Figure 5f−h). Interestingly, the $3H_2O$ configuration could suddenly reduce the barrier to 0.08 eV (Figure 5i). A close look into the configurations reveals that inserting a third H_2O molecule could naturally form H-bonding not only between the adjacent H_2O molecules but also to the surface bridging O atom (Figure 5h), which consequently assists the water splitting as follows: the inserted H_2O first releases a H atom to the surface O atom, forming an OH_b; then, a H atom of a Ti^{4+}-bound H_2O molecule transfers to the inserted one and leaves the OH_t at the Ti^{4+} site. But clearly, the PES implies the reverse recombination is more preferred (red profile in Figure 5i). These processes are akin to the H atom relay reaction at Cu(110)[4] and the theory-predicted solvent-assisted proton transfer at the H_2O/anatase-TiO_2(101) interface.[57] The reverse breaking and re-forming processes indicate a similar "pseudodissociated" state of H_2O as recognized at the Ti^{4+} site

https://doi.org/10.1021/jacs.2c03690
J. Am. Chem. Soc. 2022, 144, 13565−13573

of the rutile-TiO_2(110) surface,[9] where the OH_b and OH_t cannot be truly separated. In this case, the GS of OH_b is not expected because the charge donation to Ti^{4+} is impossible.

Further considering the photoexcited hole in the PES can reasonably fulfill the H_2O splitting: by removing only 0.2 e^- (i.e., injecting 0.2 h^+) from the $1b_1$ orbital of the Ti^{4+}-bound H_2O, we find the energy barrier is largely reduced (orange profile in Figure 5i and Figure S11) and becomes completely exothermic with 0.3 h^+ (purple profile in Figure 5i). Quite similar to the case on rutile-TiO_2(110), hole oxidation produces the radical-like $^{\bullet}OH_t$ through $H_2O + h^+ + O_b^{2-} \rightarrow {}^{\bullet}OH_t + OH_b^-$, where O_b^{2-} is the bridging surface O site.[14,15] The radical feature of $^{\bullet}OH_t$ makes it quite mobile and reactive. Meanwhile, the leaving OH_b^- with an excess electron could contribute to the GS as calculated in Figure 4b,d. From the calculated pDOS, it is found that the ridge O atoms contribute to the VBM and the terrace O atoms contribute to much deeper valence bands (Figure S12), consistent with a previous study by Xiong et al.[58] Nevertheless, the 21.2 eV light used in UPS experiments could certainly excite deep holes at the terrace O sites. It also suggests the UV and X-ray light used in UPS/XPS measurements may cause reactions that cannot be overlooked. Upon the formation of a H-bond network, hole transfer from terrace O to Ti^{4+}-bound H_2O can be coupled to the release of H in the reverse direction. Such proton-coupled hole transfer has been widely discussed on other water/oxide interfaces to understand the large overpotential for oxygen evolution in water splitting,[59−61] and we propose the H-bond network can extend this process among adjacent molecules. Future molecular dynamical calculations may help to understand whether the proton and hole transfer are concerted or sequential when proceeding through the interface and between adjacent molecules. On the rutile TiO_2 surfaces, there is no direct evidence that the H-bond network promoted the photoexcited process so far. Considering that the H-bond could assist the hole transfer and proton transfer on the rutile surface,[7,25] one may expect that the role of the H-bond network on anatase-TiO_2(001)-(1×4) should similarly participate in the case of rutile-TiO_2 surfaces. However, their different surface structures may be another effect that should be further considered.

CONCLUSION

In summary, our study provides the first observation of photoexcited water splitting at the anatase-TiO_2(001)-(1×4) surface. Although the activity of ridge sites of anatase-TiO_2(001) is still elusive, we demonstrate that the vast terrace could be a non-negligible platform for photoexcited water splitting. Different from the spontaneous H_2O dissociation at ridge sites that is activated by breaking a lattice Ti−O bond, the H_2O splitting at terrace sites is activated by the photoexcited hole. Hole oxidation produces an OH_b^- and a radical-like $^{\bullet}OH_t$ at terrace sites, and the former one contributes to the formation of a Ti^{3+} gap state. Because the terrace sites are much closer to the unreconstructed (1×1) surface on the synthesized TiO_2 nano- and microcrystals for catalytic applications, our understanding provides practical significance for TiO_2-based photocatalysis. More importantly, besides the much-concerned external activity from the TiO_2 catalyst, we emphasize that the internal H-bond network is also indispensable for water splitting, which can not only lower the dissociation energy barrier but also assist the coupled hole and proton transfer. Although our study was conducted at low temperature and under vacuum, the molecular-level understanding of water interaction and splitting on the TiO_2 surface could provide meaningful insights to the cases at room temperature and in aqueous environments. In particular, the role of the H-bond network revealed here could be a paradigm for water splitting, since it is ubiquitous in practical photocatalysis.

ASSOCIATED CONTENT

Supporting Information

The Supporting Information is available free of charge at https://pubs.acs.org/doi/10.1021/jacs.2c03690.

Sample preparation; UPS, XPS, ARPES, and STM measurements; DFT calculation details; full and zoom-in UPS spectral features; work function change with H_2O adsorption; temperature-dependent adsorption of water at the anatase-TiO_2(001)-(1×4) surface; XPS peak fitting of O 1s spectra at the anatase-TiO_2(001) surface; extracting the 1π and 3σ contributions of hydroxyl groups in UPS spectra; lattice distortion around OH_b at the terrace sites; $3a_1$ peak splitting in 2D energy-momentum space; additional STM images of H_2O at the anatase-TiO_2(001)-(1×4) surface obtained at 80 K; proposed H_2O configurations and adsorption energies; AIMD simulations; energy change of the transition state and split state by injecting holes; calculated total and partial DOS for valence bands of the anatase-TiO_2(001)-(1×4) surface (PDF)

AUTHOR INFORMATION

Corresponding Authors

Shijing Tan − *Hefei National Research Center for Physical Sciences at the Microscale and Synergetic Innovation Center of Quantum Information & Quantum Physics, University of Science and Technology of China, Hefei, Anhui 230026, China; Hefei National Laboratory, University of Science and Technology of China, Hefei 230088, China;* orcid.org/0000-0002-8537-9528; Email: tansj@ustc.edu.cn

Jin Zhao − *Hefei National Research Center for Physical Sciences at the Microscale and Synergetic Innovation Center of Quantum Information & Quantum Physics and ICQD/Hefei National Research Center for Physical Sciences at the Microscale, and CAS Key Laboratory of Strongly-Coupled Quantum Matter Physics, and Department of Physics, University of Science and Technology of China, Hefei, Anhui 230026, China;* orcid.org/0000-0003-1346-5280; Email: zhaojin@ustc.edu.cn

Bing Wang − *Hefei National Research Center for Physical Sciences at the Microscale and Synergetic Innovation Center of Quantum Information & Quantum Physics, University of Science and Technology of China, Hefei, Anhui 230026, China; Hefei National Laboratory, University of Science and Technology of China, Hefei 230088, China;* orcid.org/0000-0002-2953-2196; Email: bwang@ustc.edu.cn

Authors

Xiaochuan Ma − *Hefei National Research Center for Physical Sciences at the Microscale and Synergetic Innovation Center of Quantum Information & Quantum Physics, University of Science and Technology of China, Hefei, Anhui 230026, China;* orcid.org/0000-0002-9936-1927

Yongliang Shi − *Center for Spintronics and Quantum Systems, State Key Laboratory for Mechanical Behavior of Materials, School of Materials Science and Engineering, Xi'an Jiaotong University, Xi'an, Shaanxi 710049, China*

Jianyi Liu − *Hefei National Research Center for Physical Sciences at the Microscale and Synergetic Innovation Center of Quantum Information & Quantum Physics, University of Science and Technology of China, Hefei, Anhui 230026, China*

Xintong Li − *Hefei National Research Center for Physical Sciences at the Microscale and Synergetic Innovation Center of Quantum Information & Quantum Physics, University of Science and Technology of China, Hefei, Anhui 230026, China*

Xuefeng Cui − *Hefei National Research Center for Physical Sciences at the Microscale and Synergetic Innovation Center of Quantum Information & Quantum Physics, University of Science and Technology of China, Hefei, Anhui 230026, China; Hefei National Laboratory, University of Science and Technology of China, Hefei 230088, China*

Complete contact information is available at: https://pubs.acs.org/10.1021/jacs.2c03690

Author Contributions

X.M. and Y.S. contributed equally.

Notes

The authors declare no competing financial interest.

■ ACKNOWLEDGMENTS

This work is supported by supported by the Strategic Priority Research Program of Chinese Academy of Sciences (XDB36020200), National Natural Science Foundation of China (21972129, 11904349, 11904353), Anhui Initiative in Quantum Information Technologies (AHY090300), the Innovation Program for Quantum Science and Technology (2021ZD0303302), and the Ministry of Science and Technology of China (2016YFA0200603).

■ REFERENCES

(1) Lewis, N. S. Light work with water. *Nature* **2001**, *414*, 589−590.
(2) Kudo, A.; Miseki, Y. Heterogeneous photocatalyst materials for water splitting. *Chem. Soc. Rev.* **2009**, *38*, 253−278.
(3) Agmon, N. The Grotthuss mechanism. *Chem. Phys. Lett.* **1995**, *244*, 456−462.
(4) Kumagai, T.; Shiotari, A.; Okuyama, H.; Hatta, S.; Aruga, T.; Hamada, I.; Frederiksen, T.; Ueba, H. H-atom relay reactions in real space. *Nat. Mater.* **2012**, *11*, 167.
(5) Meng, X.; Guo, J.; Peng, J.; Chen, J.; Wang, Z.; Shi, J.-R.; Li, X.-Z.; Wang, E.-G.; Jiang, Y. Direct visualization of concerted proton tunnelling in a water nanocluster. *Nat. Phys.* **2015**, *11*, 235.
(6) Nagasaka, M.; Kondoh, H.; Amemiya, K.; Ohta, T.; Iwasawa, Y. Proton Transfer in a Two-Dimensional Hydrogen-Bonding Network: Water and Hydroxyl on a Pt(111) Surface. *Phys. Rev. Lett.* **2008**, *100*, 106101.
(7) Tan, S.; Feng, H.; Zheng, Q.; Cui, X.; Zhao, J.; Luo, Y.; Yang, J.; Wang, B.; Hou, J. G. Interfacial Hydrogen-Bonding Dynamics in Surface-Facilitated Dehydrogenation of Water on TiO_2(110). *J. Am. Chem. Soc.* **2020**, *142*, 826−834.
(8) Li, S.-C.; Chu, L.-N.; Gong, X.-Q.; Diebold, U. Hydrogen Bonding Controls the Dynamics of Catechol Adsorbed on a TiO_2(110) Surface. *Science* **2010**, *328*, 882−884.
(9) Wendt, S.; Matthiesen, J.; Schaub, R.; Vestergaard, E. K.; Lægsgaard, E.; Besenbacher, F.; Hammer, B. Formation and Splitting of Paired Hydroxyl Groups on Reduced TiO_2(110). *Phys. Rev. Lett.* **2006**, *96*, 066107.
(10) Du, Y.; Deskins, N. A.; Zhang, Z.; Dohnálek, Z.; Dupuis, M.; Lyubinetsky, I. Two Pathways for Water Interaction with Oxygen Adatoms on TiO_2(110). *Phys. Rev. Lett.* **2009**, *102*, 096102.
(11) Bikondoa, O.; Pang, C. L.; Ithnin, R.; Muryn, C. A.; Onishi, H.; Thornton, G. Direct visualization of defect-mediated dissociation of water on TiO_2(110). *Nat. Mater.* **2006**, *5*, 189−192.
(12) Donadio, D.; Ghiringhelli, L. M.; Delle Site, L. Autocatalytic and Cooperatively Stabilized Dissociation of Water on a Stepped Platinum Surface. *J. Am. Chem. Soc.* **2012**, *134*, 19217−19222.
(13) Shin, H. J.; Jung, J.; Motobayashi, K.; Yanagisawa, S.; Morikawa, Y.; Kim, Y.; Kawai, M. State-selective dissociation of a single water molecule on an ultrathin MgO film. *Nat. Mater.* **2010**, *9*, 442−447.
(14) Tan, S. J.; Feng, H.; Ji, Y. F.; Wang, Y.; Zhao, J.; Zhao, A. D.; Wang, B.; Luo, Y.; Yang, J. L.; Hou, J. G. Observation of Photocatalytic Dissociation of Water on Terminal Ti Sites of TiO_2(110)-1 × 1 Surface. *J. Am. Chem. Soc.* **2012**, *134*, 9978−9985.
(15) Migani, A.; Blancafort, L. What Controls Photocatalytic Water Oxidation on Rutile TiO_2(110) under Ultra-High-Vacuum Conditions? *J. Am. Chem. Soc.* **2017**, *139*, 11845−11856.
(16) Fujishima, A.; Zhang, X. T.; Tryk, D. A. TiO_2 photocatalysis and related surface phenomena. *Surf. Sci. Rep.* **2008**, *63*, 515−582.
(17) Rahman, M. Z.; Edvinsson, T.; Gascon, J. Hole utilization in solar hydrogen production. *Nat. Rev. Chem.* **2022**, *6*, 243−258.
(18) Henderson, M. A. A surface science perspective on TiO_2 photocatalysis. *Surf. Sci. Rep.* **2011**, *66*, 185−297.
(19) Migani, A.; Mowbray, D. J.; Zhao, J.; Petek, H.; Rubio, A. Quasiparticle Level Alignment for Photocatalytic Interfaces. *J. Chem. Theor. Comp.* **2014**, *10*, 2103−2113.
(20) Sun, H.; Mowbray, D. J.; Migani, A.; Zhao, J.; Petek, H.; Rubio, A. Comparing Quasiparticle H_2O Level Alignment on Anatase and Rutile TiO_2. *ACS Catal.* **2015**, *5*, 4242−4254.
(21) Di Valentin, C.; Selloni, A. Bulk and Surface Polarons in Photoexcited Anatase TiO_2. *J. Phys. Chem. Lett.* **2011**, *2*, 2223−2228.
(22) Zawadzki, P.; Laursen, A. B.; Jacobsen, K. W.; Dahl, S.; Rossmeisl, J. Oxidative trends of TiO_2—hole trapping at anatase and rutile surfaces. *Energy Environ. Sci.* **2012**, *5*, 9866−9869.
(23) Zhang, H.; Zhou, P.; Chen, Z.; Song, W.; Ji, H.; Ma, W.; Chen, C.; Zhao, J. Hydrogen-Bond Bridged Water Oxidation on {001} Surfaces of Anatase TiO_2. *J. Phys. Chem. C* **2017**, *121*, 2251−2257.
(24) Setvin, M.; Shi, X.; Hulva, J.; Simschitz, T.; Parkinson, G. S.; Schmid, M.; Di Valentin, C.; Selloni, A.; Diebold, U. Methanol on Anatase TiO_2(101): Mechanistic Insights into Photocatalysis. *ACS Catal.* **2017**, *7*, 7081−7091.
(25) Chu, W.; Tan, S.; Zheng, Q.; Fang, W.; Feng, Y.; Prezhdo, O. V.; Wang, B.; Li, X.-Z.; Zhao, J. Ultrafast charge transfer coupled to quantum proton motion at molecule/metal oxide interface. *Sci. Adv.* **2022**, *8*, eabo2675.
(26) Yang, W.; Wei, D.; Jin, X.; Xu, C.; Geng, Z.; Guo, Q.; Ma, Z.; Dai, D.; Fan, H.; Yang, X. Effect of the Hydrogen Bond in Photoinduced Water Dissociation: A Double-Edged Sword. *J. Phys. Chem. Lett.* **2016**, *7*, 603−608.
(27) Xu, C.; Xu, F.; Chen, X.; Li, Z.; Luan, Z.; Wang, X.; Guo, Q.; Yang, X. Wavelength-Dependent Water Oxidation on Rutile TiO_2(110). *J. Phys. Chem. Lett.* **2021**, *12*, 1066−1072.
(28) Hussain, H.; Tocci, G.; Woolcot, T.; Torrelles, X.; Pang, C. L.; Humphrey, D. S.; Yim, C. M.; Grinter, D. C.; Cabailh, G.; Bikondoa, O.; Lindsay, R.; Zegenhagen, J.; Michaelides, A.; Thornton, G. Structure of a model TiO_2 photocatalytic interface. *Nat. Mater.* **2017**, *16*, 461−466.
(29) Kamal, C.; Stenberg, N.; Walle, L. E.; Ragazzon, D.; Borg, A.; Uvdal, P.; Skorodumova, N. V.; Odelius, M.; Sandell, A. Core-Level Binding Energy Reveals Hydrogen Bonding Configurations of Water Adsorbed on TiO_2(110) Surface. *Phys. Rev. Lett.* **2021**, *126*, 016102.
(30) Yim, C.; Pang, C.; Thornton, G. Oxygen Vacancy Origin of the Surface Band-Gap State of TiO_2(110). *Phys. Rev. Lett.* **2010**, *104*, 036806.

(31) Wendt, S.; Sprunger, P. T.; Lira, E.; Madsen, G. K. H.; Li, Z.; Hansen, J. O.; Matthiesen, J.; Blekinge-Rasmussen, A.; Laegsgaard, E.; Hammer, B.; Besenbacher, F. The Role of Interstitial Sites in the Ti3*d* Defect State in the Band Gap of Titania. *Science* **2008**, *320*, 1755−1759.
(32) Di Valentin, C.; Pacchioni, G.; Selloni, A. Electronic structure of defect states in hydroxylated and reduced rutile TiO_2(110) surfaces. *Phys. Rev. Lett.* **2006**, *97*, 166803.
(33) Diebold, U. The surface sience of titanium dioxide. *Surf. Sci. Rep.* **2003**, *48*, 53−229.
(34) Minato, T.; Sainoo, Y.; Kim, Y.; Kato, H. S.; Aika, K.-i.; Kawai, M.; Zhao, J.; Petek, H.; Huang, T.; He, W.; Wang, B.; Wang, Z.; Zhao, Y.; Yang, J.; Hou, J. G. The electronic structure of oxygen atom vacancy and hydroxyl impurity defects on titanium dioxide (110) surface. *J. Chem. Phys.* **2009**, *130*, 124502.
(35) Lazzeri, M.; Vittadini, A.; Selloni, A. Structure and energetics of stoichiometric TiO_2 anatase surfaces. *Phys. Rev. B* **2001**, *63*, 155409.
(36) Gong, X.-Q.; Selloni, A.; Vittadini, A. Density Functional Theory Study of Formic Acid Adsorption on Anatase TiO_2(001): Geometries, Energetics, and Effects of Coverage, Hydration, and Reconstruction. *J. Phys. Chem. B* **2006**, *110*, 2804−2811.
(37) Yang, H. G.; Sun, C. H.; Qiao, S. Z.; Zou, J.; Liu, G.; Smith, S. C.; Cheng, H. M.; Lu, G. Q. Anatase TiO_2 single crystals with a large percentage of reactive facets. *Nature* **2008**, *453*, 638−641.
(38) Pei, D.-N.; Gong, L.; Zhang, A.-Y.; Zhang, X.; Chen, J.-J.; Mu, Y.; Yu, H.-Q. Defective titanium dioxide single crystals exposed by high-energy {001} facets for efficient oxygen reduction. *Nat. Commun.* **2015**, *6*, 8696.
(39) Lazzeri, M.; Selloni, A. Stress-driven reconstruction of an oxide surface: The anatase TiO_2(001)-(1 × 4) surface. *Phys. Rev. Lett.* **2001**, *87*, 266105.
(40) Wang, Y.; Sun, H.; Tan, S.; Feng, H.; Cheng, Z.; Zhao, J.; Zhao, A.; Wang, B.; Luo, Y.; Yang, J.; Hou, J. G. Role of point defects on the reactivity of reconstructed anatase titanium dioxide (001) surface. *Nat. Commun.* **2013**, *4*, 2214.
(41) Yuan, W.; Wang, Y.; Li, H.; Wu, H.; Zhang, Z.; Selloni, A.; Sun, C. Real-Time Observation of Reconstruction Dynamics on TiO_2(001) Surface under Oxygen via an Environmental Transmission Electron Microscope. *Nano Lett.* **2016**, *16*, 132−137.
(42) Beinik, I.; Bruix, A.; Li, Z.; Adamsen, K. C.; Koust, S.; Hammer, B.; Wendt, S.; Lauritsen, J. V. Water Dissociation and Hydroxyl Ordering on Anatase TiO_2(001)-(1 × 4). *Phys. Rev. Lett.* **2018**, *121*, 206003.
(43) Vittadini, A.; Casarin, M.; Selloni, A. Chemistry of and on TiO_2-anatase surfaces by DFT calculations: a partial review. *Theor. Chem. Acc.* **2007**, *117*, 663−671.
(44) Blomquist, J.; Walle, L. E.; Uvdal, P.; Borg, A.; Sandell, A. Water Dissociation on Single Crystalline Anatase TiO_2(001) Studied by Photoelectron Spectroscopy. *J. Phys. Chem. C* **2008**, *112*, 16616−16621.
(45) Shi, Y.; Sun, H.; Nguyen, M. C.; Wang, C.; Ho, K.; Saidi, W. A.; Zhao, J. Structures of defects on anatase TiO_2(001) surfaces. *Nanoscale* **2017**, *9*, 11553−11565.
(46) Xiong, F.; Yin, L.-L.; Li, F.; Wu, Z.; Wang, Z.; Sun, G.; Xu, H.; Chai, P.; Gong, X.-Q.; Huang, W. Anatase TiO_2(001)-(1 × 4) Surface Is Intrinsically More Photocatalytically Active than the Rutile TiO_2(110)-(1 × 1) Surface. *J. Phys. Chem. C* **2019**, *123*, 24558−24565.
(47) Yuan, W.; Zhu, B.; Li, X.-Y.; Hansen, T. W.; Ou, Y.; Fang, K.; Yang, H.; Zhang, Z.; Wagner, J. B.; Gao, Y.; Wang, Y. Visualizing H_2O molecules reacting at TiO_2 active sites with transmission electron microscopy. *Science* **2020**, *367*, 428−430.
(48) Sun, H.; Lu, W.; Zhao, J. Structure and Reactivity of Anatase TiO_2(001)-(1 × 4) Surface. *J. Phys. Chem. C* **2018**, *122*, 14528−14536.
(49) Shi, Y.; Sun, H.; Saidi, W. A.; Nguyen, M. C.; Wang, C. Z.; Ho, K.; Yang, J.; Zhao, J. Role of Surface Stress on the Reactivity of Anatase TiO_2(001). *J. Phys. Chem. Lett.* **2017**, *8*, 1764−1771.
(50) Henderson, M. A. The interaction of water with solid surfaces: fundamental aspects revisited. *Surf. Sci. Rep.* **2002**, *46*, 1−308.
(51) Tzvetkov, G.; Zubavichus, Y.; Koller, G.; Schmidt, T.; Heske, C.; Umbach, E.; Grunze, M.; Ramsey, M.; Netzer, F. Growth of H_2O layers on an ultra-thin Al_2O_3 film: from monomeric species to ice. *Surf. Sci.* **2003**, *543*, 131−140.
(52) Bigi, C.; Tang, Z.; Pierantozzi, G. M.; Orgiani, P.; Das, P. K.; Fujii, J.; Vobornik, I.; Pincelli, T.; Troglia, A.; Lee, T.-L.; Ciancio, R.; Drazic, G.; Verdini, A.; Regoutz, A.; King, P. D. C.; Biswas, D.; Rossi, G.; Panaccione, G.; Selloni, A. Distinct behavior of localized and delocalized carriers in anatase TiO_2(001) during reaction with O_2. *Phys. Rev. Mater.* **2020**, *4*, 025801.
(53) Ma, X.; Cheng, Z.; Tian, M.; Liu, X.; Cui, X.; Huang, Y.; Tan, S.; Yang, J.; Wang, B. Formation of Plasmonic Polarons in Highly Electron-Doped Anatase TiO_2. *Nano Lett.* **2021**, *21*, 430−436.
(54) Tang, H.; Cheng, Z.; Dong, S.; Cui, X.; Feng, H.; Ma, X.; Luo, B.; Zhao, A.; Zhao, J.; Wang, B. Understanding the Intrinsic Chemical Activity of Anatase TiO_2(001)-(1 × 4) Surface. *J. Phys. Chem. C* **2017**, *121*, 1272−1282.
(55) Nordlund, D.; Odelius, M.; Bluhm, H.; Ogasawara, H.; Pettersson, L. G. M.; Nilsson, A. Electronic structure effects in liquid water studied by photoelectron spectroscopy and density functional theory. *Chem. Phys. Lett.* **2008**, *460*, 86−92.
(56) Selçuk, S.; Selloni, A. Surface Structure and Reactivity of Anatase TiO_2 Crystals with Dominant {001} Facets. *J. Phys. Chem. C* **2013**, *117*, 6358−6362.
(57) Calegari Andrade, M. F.; Ko, H.-Y.; Zhang, L.; Car, R.; Selloni, A. Free energy of proton transfer at the water−TiO_2 interface from ab initio deep potential molecular dynamics. *Chem. Sci.* **2020**, *11*, 2335−2341.
(58) Xiong, F.; Yin, L.-L.; Wang, Z.; Jin, Y.; Sun, G.; Gong, X.-Q.; Huang, W. Surface Reconstruction-Induced Site-Specific Charge Separation and Photocatalytic Reaction on Anatase TiO_2(001) Surface. *J. Phys. Chem. C* **2017**, *121*, 9991−9999.
(59) Chen, J.; Li, Y.-F.; Sit, P.; Selloni, A. Chemical Dynamics of the First Proton-Coupled Electron Transfer of Water Oxidation on TiO_2 Anatase. *J. Am. Chem. Soc.* **2013**, *135*, 18774−18777.
(60) Cheng, J.; Liu, X.; Kattirtzi, J. A.; VandeVondele, J.; Sprik, M. Aligning Electronic and Protonic Energy Levels of Proton-Coupled Electron Transfer in Water Oxidation on Aqueous TiO_2. *Angew. Chem., Int. Ed.* **2014**, *53*, 12046−12050.
(61) Ji, Y.; Wang, B.; Luo, Y. A Comparative Theoretical Study of Proton-Coupled Hole Transfer for H_2O and Small Organic Molecules (CH_3OH, HCOOH, H_2CO) on the Anatase TiO_2(101) Surface. *J. Phys. Chem. C* **2014**, *118*, 21457−21462.

https://doi.org/10.1021/jacs.2c03690
J. Am. Chem. Soc. 2022, 144, 13565−13573